



HAL
open science

Modification by high energy ion irradiation of iron-alumina nano-composites.

Christophe Laurent, Eric Dooryhée, Christian Dufour, Fabrice Gourbilleau,
Marc Levalois, Gérard Nouet, E. Paumier

► **To cite this version:**

Christophe Laurent, Eric Dooryhée, Christian Dufour, Fabrice Gourbilleau, Marc Levalois, et al..
Modification by high energy ion irradiation of iron-alumina nano-composites.. Nuclear Instruments
and Methods in Physics Research Section B: Beam Interactions with Materials and Atoms, 1996, 107
(1-4), pp.232-238. 10.1016/0168-583X(95)01033-5 . hal-03485466

HAL Id: hal-03485466

<https://hal.science/hal-03485466>

Submitted on 17 Dec 2021

HAL is a multi-disciplinary open access archive for the deposit and dissemination of scientific research documents, whether they are published or not. The documents may come from teaching and research institutions in France or abroad, or from public or private research centers.

L'archive ouverte pluridisciplinaire **HAL**, est destinée au dépôt et à la diffusion de documents scientifiques de niveau recherche, publiés ou non, émanant des établissements d'enseignement et de recherche français ou étrangers, des laboratoires publics ou privés.



Open Archive TOULOUSE Archive Ouverte (OATAO)

OATAO is an open access repository that collects the work of Toulouse researchers and makes it freely available over the web where possible.

This is an author-deposited version published in : <http://oatao.univ-toulouse.fr/> Eprints
ID : 11167

To link to this article : DOI:10.1016/0168-583X(95)01033-5

URL : [http://dx.doi.org/10.1016/0168-583X\(95\)01033-5](http://dx.doi.org/10.1016/0168-583X(95)01033-5)

To cite this version :

Laurent, Christophe and Dooryh e, Eric and Dufour, Christian and Gourbilleau, Fabrice and Levalois, M. and Nouet, G erard and Paumier, E. *Modification by high energy ion irradiation of iron-alumina nano-composites*. (1996) Nuclear Instruments and Methods in Physics Research Section B: Beam Interactions with Materials and Atoms, vol. 107 (n  1-4). pp. 232-238. ISSN 0168-583X

Any correspondance concerning this service should be sent to the repository administrator: staff-oatao@listes-diff.inp-toulouse.fr

Modification by high energy ion irradiation of iron–alumina nano-composites ¹

Ch. Laurent ^a, E. Dooryhée ^{b,*}, C. Dufour ^c, F. Gourbilleau ^c, M. Levalois ^{b,c}, G. Nouet ^c,
E. Paumier ^{b,c}

^a LCMI, URA CNRS 1311, Université Paul Sabatier, 31062 Toulouse Cedex, France

^b CIRIL, CEA-CNRS, rue Claude Bloch, BP 5133, 14040 Caen Cedex, France

^c LERMAT, URA CNRS 1317, ISMRA, 6 Bd du Maréchal Juin, 14050 Caen, France

Abstract

This work reports on the current observations by transmission electron microscopy (TEM) of nano-composites irradiated by GeV heavy ions. The composite targets consist of nanometric Fe particles dispersed in a ceramic (Al₂O₃) powder. Large metal particles (~ 30 nm diameter) are located over the alumina grain surface whereas smaller particles (~ 10 nm) are directly epitaxied in the alumina grains. The TEM micrographs show that the surface distribution of the large particles and the orientation of the small Fe particles in the Al₂O₃ micrometer grains are changed by the irradiation. At high fluences, the grains of alumina are destroyed.

1. Introduction

The imaging by transmission electron microscopy (TEM) has provided a major insight into the atomic details of the structural changes produced in a solid by swift heavy ion irradiation (SHI) [1–6]. Over the past years, the TEM studies have rather focused on the SHI effects in *bulk* solids which are not sensitive to purely ionizing radiations (photons or electrons). For example, TEM has revealed the formation of latent tracks in high T_c superconductors such as YBa₂Cu₃O₇ [7], the amorphization of NiZr₂ [8] or the phase change in Ti [9]. The description of the effects along the ion path (point defects, clusters of defects, amorphization, strain) was largely improved in Y₃Fe₅O₁₂, BaFe₁₂O₁₉ and other ferrimagnetic oxides [6,10].

The present work reports on the first TEM observations of SHI effects in an alumina based nano-composite. The novel target investigated in the present study consists of nanometric iron particles dispersed in and over the micrometer-sized grains of powdered α -Al₂O₃. Both materials (Fe and Al₂O₃) are highly resistant to low densities of electronic excitations, and the effects of swift heavy ion

irradiation (SHI) in *bulk* Fe and Al₂O₃ have been the object of recent investigations. SHI produces an important lattice disorder in monocrystalline α -Al₂O₃, in relation with the high densities of electronic excitations [11]. For $dE/dx \leq 4$ keV/Å, the amount of damage in pure polycrystalline Fe is smaller than what results from nuclear collisions only [12]. For $dE/dx \geq 4$ keV/Å, a strong enhancement of the damage is observed in Fe, due to electronic excitations [12]. We are now investigating the response to SHI of nanometric iron dispersed in an insulating alumina matrix.

Interest in the response of the Fe–Al₂O₃ nano-composite to SHI is further stimulated by recent observations in Na–MgO [13]: sodium dispersoids (~ 10 nm diameter) embedded in a MgO single crystal vanish away under SHI. The decrease of the concentration of the alkali nano-precipitates in the MgO matrix is imparted to a SHI induced atomic mixing at the Na/MgO interface. In the present article, the TEM micrographs depict the evolution of the Fe–Al₂O₃ nano-structure under SHI. The distribution of the Fe nano-particles (location, orientation, size and concentration) and the stability of the composite are observed after SHI. The large densities of electronic excitations produced by the incident GeV heavy ions are responsible for the observed features. These unique modifications in turn could affect the related properties of Fe–Al₂O₃ such as the mechanical strengthening and the super-paramagnetism.

¹ Ion irradiation performed at the GANIL accelerator, Caen, France.

* Corresponding author. Fax (+33) 31 45 47 14, tel. (+33) 31 45 47 54, e-mail: dooryhee@ganac4.in2p3.fr.

2. Experimental

2.1. Sample preparation and characterization

The 20 wt.% Fe–Al₂O₃ nano-composite powder was prepared according to the method proposed by Devaux et al. [14]. The mixed complex oxalate (NH₄)₃[Al_{1.8}Fe_{0.2}(C₂O₄)₃] was prepared by co-precipitation of aluminium and iron oxalates. The mixed oxalate was decomposed in air at 673 K and next calcinated in air at 1373 K, yielding an intimate mixture of two mixed oxide phases as shown by X-ray diffraction (XRD). The major phase is an Al-rich solid solution of the α -Al₂O₃ (corundum) type, whereas the minor phase is an Fe-rich solid solution of the α -Fe₂O₃ (hematite) type. The latter phase forms because the solubility of hematite in α -Al₂O₃ is limited to 10 wt.% [15]. The oxide powder was heated up at 1573 K in pure, dry hydrogen for 1 h, giving rise to the 20 wt.% Fe–Al₂O₃ nano-composite powder. It is studied by XRD and Mössbauer spectroscopy.

The microstructure of the specimens was investigated using transmission electron microscopy (TEM) and related techniques such as electron micro-diffraction (ED) and energy-dispersive X-ray analysis (EDS).

2.2. Irradiation conditions

The Fe–Al₂O₃ powder was laid and dried out over a 400 mesh copper grid after ultrasonic dispersion in ethanol. Each grid was observed by TEM as irradiated. The grids covered with powder were exposed to 1 GeV ¹⁸¹Ta ions (incident energy $E = 5.7$ MeV/amu) at 80 K. The stopping power of Ta is dominated by inelastic interactions.

The electronic energy loss dE/dx is 5.4 and 3.6 keV/Å in Fe and Al₂O₃ respectively. It exceeds the energy loss by elastic collisions by more than a factor 600. The fluences are 1.5×10^{12} (#1), 3×10^{12} (#2) and 10^{13} cm⁻² (specimen #3). The particle flux was limited to $\sim 2 \times 10^8$ cm⁻² s⁻¹ for preventing any excessive heating.

3. Results

3.1. Non-irradiated powder

XRD analysis of the nano-composite powder reveals the presence of metallic iron and α -Al₂O₃ only. The reduction treatment was made at a temperature high enough to avoid the formation of a FeAl₂O₄ spinel phase [16]. Analysis of the Mössbauer spectra shows the absence of ferrous and ferric ions, thus confirming that the reduction is total at 1573 K [17]. The intra-granular Fe particles are formed by reduction of the substitutional Fe³⁺ ions in the Al-rich solid solution. The ferromagnetic surface Fe particles derive from the reduction of the Fe-rich zones and from the coalescence of smaller particles by diffusion at the surface and in the open porosity of the matrix [14,17]. TEM observations (Fig. 1) show the microstructure of the composite powder. The dimensions of the matrix grains are of the order of a few hundreds of nanometers. The EDS analyses confirm the global iron content (20 wt.%). Most of the Fe particles are smaller than 10 nm in size and uniformly located inside the alumina grains. Some larger (≤ 30 nm) metal particles are located at the surface and in the open porosity of the oxide matrix. A previous study

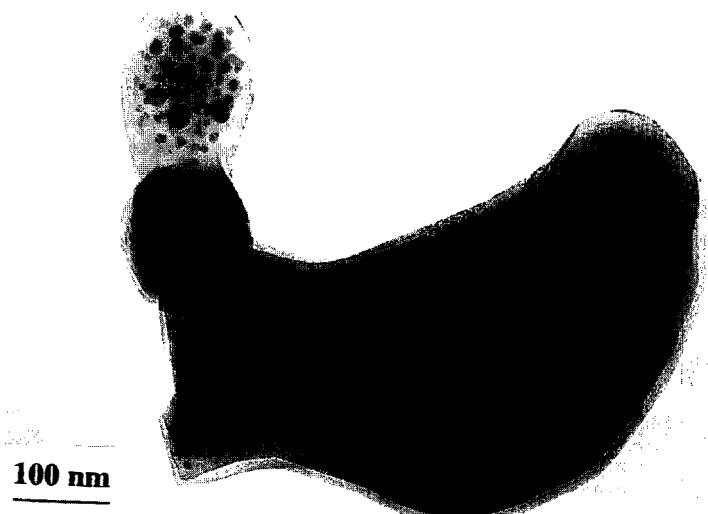


Fig. 1. TEM micrograph of the non-irradiated 20 wt.% Fe–Al₂O₃ powder. The μ m-size alumina mono-crystalline grain contains a uniform distribution of nano-crystalline, epitaxied Fe precipitates (~ 10 nm size). Larger Fe particles (~ 30 nm) are observed over the surface of the alumina grain.

[18] has shown that both the alumina grains and the Fe particles are monocrystalline and that the intra-granular Fe particles are epitaxially oriented in the alumina lattice according to the following general epitaxial relationship:

$$(111)[\bar{1}\bar{1}2]_{\text{Fe}} \parallel (0001)[10\bar{1}0]_{\alpha\text{-Al}_2\text{O}_3}$$

3.2. Latent tracks in irradiated specimens

TEM observations of specimen #1 reveals the presence of tracks of cylindrical morphology, parallel to each other in an alumina grain (Fig. 2a). The diameter of a cylinder is approximately 2 nm. Such tracks are also observed in the other specimens, but a strong carbon contamination occurring under the electron beam impairs the quality of the TEM micrographs. Crack-like, cylindrical defects much

shorter than those described above are also observed in specimen #1 (Fig. 2b). It is noteworthy that there is an area where a much lower concentration of Fe particles is observed. The edge and some features of the alumina grain in this area look "rounded".

It should be noted that "doublet" tracks similar to those observed in Cr-Al₂O₃ nano-composite powder irradiated with 3.7 MeV/amu ¹⁵⁴Sm ions [19] were not detected in the present specimens.

3.3. Evolution of the nano-structure in irradiated specimens

A comparison of the ED patterns before (Fig. 3a) and after irradiation (Figs. 3b-3d) shows that the intra-granular Fe particles do no longer share the same orientation after

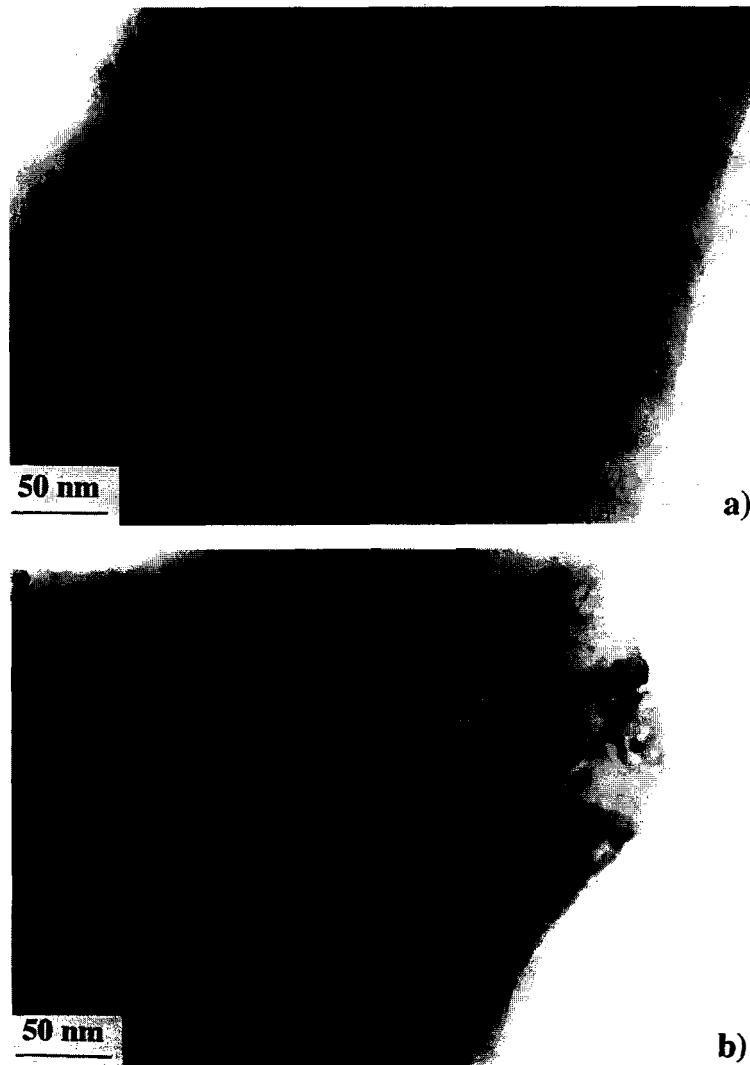


Fig. 2. TEM micrographs showing (a) tracks (diameter \approx 2 nm) and (b) cracks in specimen #1 (fluence = 1.5×10^{12} Ta/cm²).

irradiation and that the magnitude of the disorientation effect increases with increasing fluence. Indeed, one can see that some extra (110) Fe diffraction spots appear on the ED pattern of specimen #1 (Fig. 3b). This is explained

by the rotation of some Fe particles away from their epitaxial position. The diffuse (110) Fe diffraction ring is detected on the ED pattern of specimen #2 (Fig. 3c), showing more and more disorientation. For specimen #3

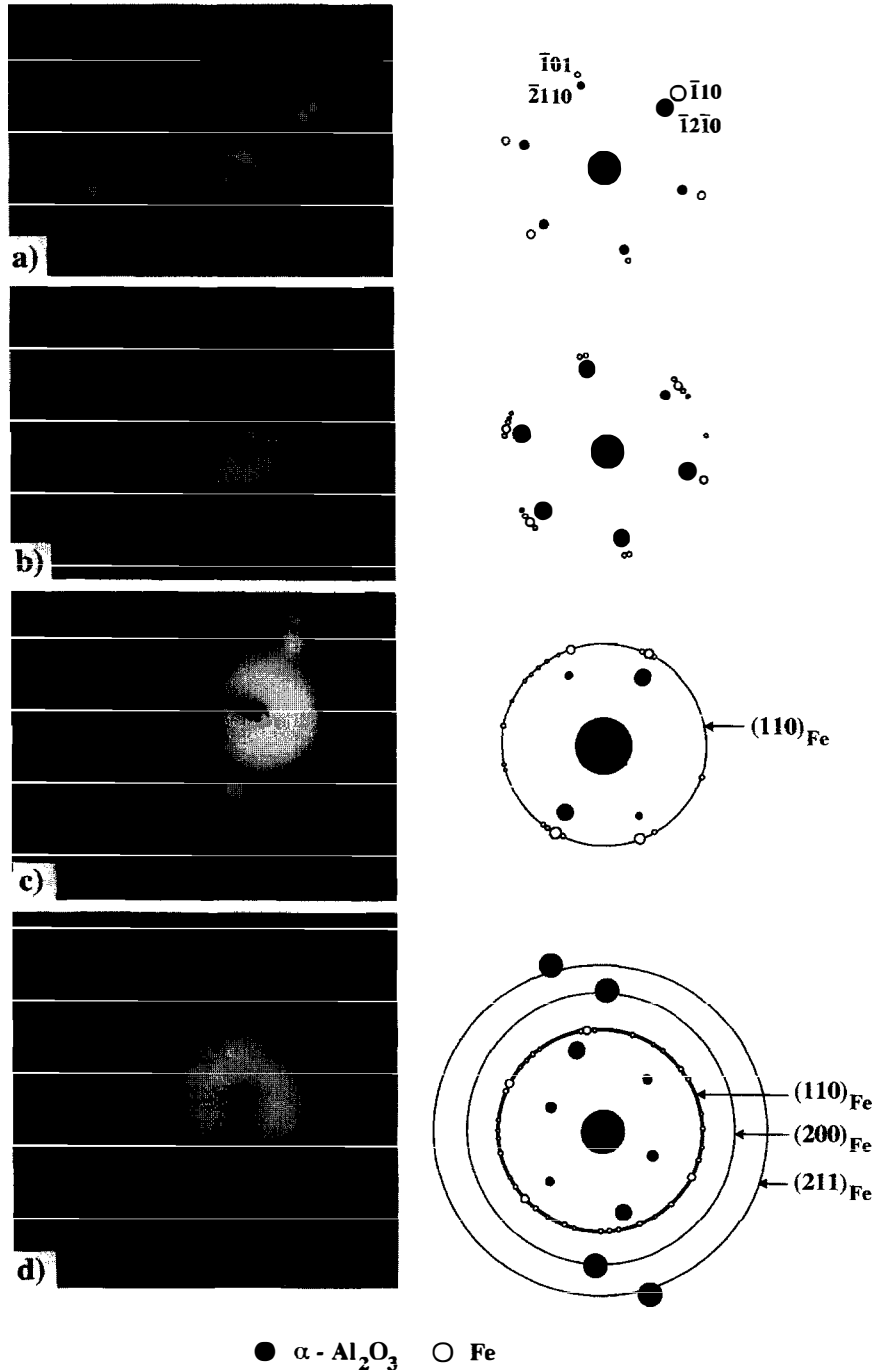


Fig. 3. ED patterns of the non-irradiated 20 wt.% Fe- Al_2O_3 powder (a), specimen #1 at 1.5×10^{12} Ta/cm² (b), #2 at 3×10^{12} Ta/cm² (c) and #3 at 10^{13} Ta/cm² (d). a) superimposed diffraction patterns of the two lattices, Fe and Al_2O_3 , sharing the same orientation. b) (110) Fe diffraction extra spots appear. c) Fe nano-particles are more and more disoriented, contributing to the (110) Fe Scherrer ring. d) (200) and (211) Fe diffraction occurs, for a single orientation of the substrate alumina grain.

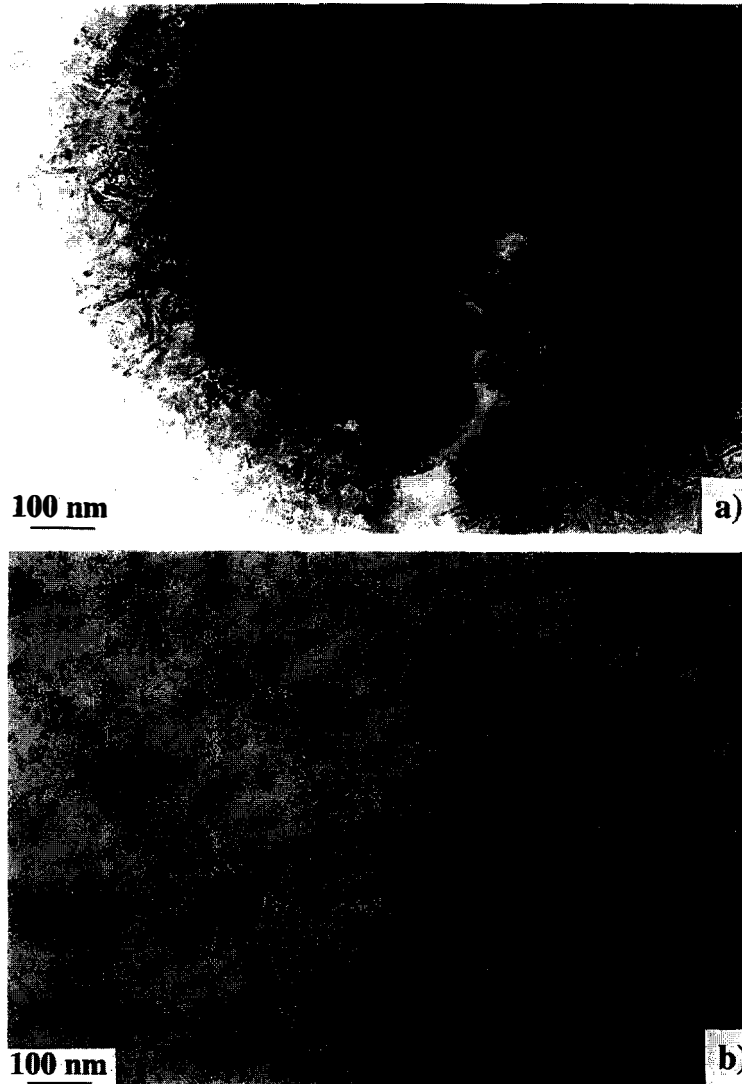


Fig. 4. TEM micrographs showing destroyed grains in specimens #2 (a) and #3 (b). The Ta fluences are $3 \times 10^{12} \text{ cm}^{-2}$ and 10^{13} cm^{-2} respectively. In specimen #2, 10 nm size fragments composed of Al and Fe are visible.

(Fig. 3d), the (110) Fe diffraction ring, with many more diffraction spots, is even more clearly detected, and the (200) Fe and (211) Fe diffraction rings are as well detected.

The destruction of some composite grains is observed in specimens #2 and #3 (Fig. 4), but not in specimen #1. It can be seen that the destruction may either be partial or total, but is not systematically related with the fluence. Thus it is not yet possible to determine whether there is a threshold fluence at which grain destruction starts or whether this is a progressive effect. EDS analyses reveal that both Al and Fe are present in the fragments; most of which are as small as 10 nm in size (Fig. 4). In the case of partial destruction, needle-shaped fragments are observed in the vicinity of the virgin grain (Fig. 4a).

EDS analyses were performed on specimen #3 during

the TEM observations. The Fe content in the grains shown in Fig. 1 is found to be approximately 7.5 wt.%. These values are measured on very small zones inside these grains and closely match the intra-granular iron content found by other methods [20]. It seems that the Fe particles located at the surface and in the open porosity of the oxide matrix are removed from their original location due to SHI.

4. Discussion

4.1. Disorientation of the Fe nano-inclusions in Al_2O_3

Stress relaxation in the alumina lattice could account for the disorientation of the Fe particles. Indeed, the most

frequently observed epitaxial relationships [21] correspond to a fairly high lattice mismatch (15–20%). It must be remembered that the intra-granular Fe particles do not grow in a free manner. Their orientation is rather dictated by the matrix, which is crystallized in the stable α -Al₂O₃ form prior to the nucleation of the metallic iron. Thus, it may be considered that stress relaxation induced by SHI allows the disorientation of the Fe inclusions into a more energetically favourable position.

4.2. Role of the elastic collisions

The contribution of elastic nuclear collisions into the process of atomic mixing or bond breaking can be readily estimated. The number of target atoms moved out by elastic knock-on is overestimated using the TRIM code [22]. For a fluence $\phi_t = 10^{12}$ Ta/cm², the computed simulation yields 3×10^{-5} vacancy per target atom (dpa) in Al₂O₃ and 7×10^{-5} dpa in Fe. An analytical treatment using the Lindhard potential [23] and the formulae of Norgett et al. [24] gives very similar values. Given a nano-particle of 10 nm diameter, no more than 6 iron atoms can be displaced away for 10^{12} Ta/cm². Nuclear collisions are by far insufficient for the creation of a mixed interface, and cannot break a sufficient number of bonds at the interface. The nuclear collisions are not responsible either for the destruction of the surface particles.

The calculated total cross section for atomic displacement by direct elastic collisions is $\sim 3 \times 10^{-17}$ cm² in pure α -Al₂O₃. Canut et al. [25] measured the fraction of disorder produced by 0.9 GeV ²⁰⁸Pb ions ($dE/dx = 4.1$ keV/Å) in monocrystalline α -Al₂O₃, by means of channeling Rutherford backscattering spectrometry. The measured total cross section for effective atomic displacement is $\sim 10^{-13}$ cm² (at 80 K). We infer from the above discussion that electronic excitations largely prevail in the process of intra-granular Fe particle rotation and in the destruction of the surface Fe particles.

4.3. Inelastic energy loss in Fe nano-particles

A crude estimate of the energy absorbed by the surface metal particle (~ 30 nm diameter) through electronic excitations yields ~ 0.7 eV/atom per hit. We calculate that 80% of the incident energy is retained within the isolated particle (50% if diameter ~ 10 nm). This accounts for the kinetic energy lost out of the particle by escaping ejected electrons. The calculation consists of intersecting the track radial profile of the energy carried away by the electrons [26] and the finite cylinder-like volume of the nano-particle [27]. For a fluence of 10^{12} cm⁻², the large particles receive 7 impacts on average (less than 1 for intra-granular particles). The value ~ 0.7 eV/atom/projectile can be tentatively compared with the thermal energy absorbed by Fe at 80 K for complete melting: 0.8 eV/atom. Due to the compressive stress in the alumina matrix, the fusion energy

of the intra-granular Fe particles is expected to be higher. Based on this thermodynamical difference, could the thermal spike model [28] explain that the large, free particles (on surface) disappear whereas the small, embedded particles (intra-granular) are still observed after SHI?

5. Conclusion

We have examined the structural modifications induced by GeV Ta ions in a nano-composite target (Fe–Al₂O₃) at 80 K. The irradiated material is composed of a powder of micrometric alumina grains, with nano-particles of Fe (20 wt.%) dispersed inside and outside the ceramic grains. The epitaxial orientation of the intra-granular Fe inclusions is progressively lost with increasing fluence. The larger Fe particles located at the surface and in the open porosity of the oxide grains disappear from their original sites. Track-like features are observed and fragmentation of the oxide grains occurs. These significant modifications mark the efficient conversion of track electronic excitations into atomic effects in materials (Fe and Al₂O₃) a priori not much sensitive to low rates of electronic excitations.

References

- [1] E.C.H. Silk and R.S. Barnes, *Philos. Mag.* 7 (1959) 970.
- [2] P.B. Price and R.M. Walker, *J. Appl. Phys.* 33 (1962) 3400.
- [3] L.A. Bursill and G. Braunshausen, *Philos. Mag. A* 62 (1990) 395.
- [4] S. Furano, K. Izui and H. Otsu, *J. Electron, Microsc.* 30 (1981) 327.
- [5] D.V. Morgan and L.T. Chadderton, *Philos. Mag.* 17 (1968) 1135.
- [6] C. Houpert, M. Hervieu, D. Groult, F. Studer and M. Toulemonde, *Nucl. Instr. and Meth. B* 32 (1988) 393; C. Houpert, F. Studer, D. Groult and M. Toulemonde, *Nucl. Instr. and Meth. B* 39 (1989) 720.
- [7] D. Bourgault, D. Groult, S. Bouffard, M. Hervieu, J. Provost, F. Studer and B. Raveau, *Radiat. Eff. and Def. in Solids* 110 (1989) 211.
- [8] A. Barbu, A. Dunlop, D. Lesueur and R.S. Averback, *Europhys. Lett.* 15 (1991) 37.
- [9] H. Dammak, A. Barbu, A. Dunlop, D. Lesueur and N. Lorenzelli, *Philos. Mag. Lett.* 67 (1993) 253.
- [10] M. Toulemonde, G. Fuchs, F. Studer, N. Nguyen and D. Groult, *Phys. Rev. B* 35 (1987) 6560.
- [11] J.M. Marty, A. Benyagoub, G. Marest, N. Moncoffre, M. Toulemonde, A. Meftah, F. Studer, B. Canut, S.M.M. Ramos and P. Thevenard, *Nucl. Instr. and Meth. B* 91 (1994) 274.
- [12] A. Dunlop, D. Lesueur, P. Legrand and H. Dammak, *Nucl. Instr. and Meth. B* 90 (1994) 330.
- [13] M. Beranger, R. Brenier, B. Canut, S.M.M. Ramos, P. Thevenard, A. Brunel, S. Della Negra, Y. Le Beyec, E. Balanzat and M. Toulemonde, presented at 9th Int. Conf. on Ion Beam Modification of Materials, Canberra, Australia, 1995.

- [14] X. Devaux, Ch. Laurent and A. Rousset, *Nanostruct. Mater.* 2 (1993) 339.
- [15] A. Muan and C.L. Gee, *J. Am. Ceram. Soc.* 39 (1955) 207.
- [16] Ch. Laurent, A. Rousset, M. Verelst, K.R. Kannan, A.R. Raju and C.N.R. Rao, *J. Mater. Chem.* 3 (1993) 513.
- [17] Ch. Laurent, J.J. Demai, A. Rousset, K.R. Kannan and C.N.R. Rao, *J. Mater. Res.* 9 (1994) 229.
- [18] X. Devaux, Ch. Laurent, M. Brieu and A. Rousset, *J. Alloys and Compounds* 188 (1992) 179.
- [19] E. Dooryhee, V. Chailley, C. Dufour, F. Gourbilleau, M. Levalois, G. Nouet, E. Paumier, Ch. Laurent and C. Monty, presented at 9th Int. Conf. on Ion Beam Modification of Materials, Canberra, Australia, 1995.
- [20] Ch. Laurent, Ph.D. thesis, Toulouse (1994).
- [21] X. Devaux, Ph.D. thesis, Toulouse (1991).
- [22] J.P. Biersack and L.G. Haggmark, *Nucl. Instr. and Meth.* 174 (1980) 257.
- [23] J. Lindhard and M. Scharff, *Phys. Rev.* 124 (1961) 128.
- [24] M.J. Norgett, M.T. Robinson and I.M. Torrens, *Nucl. Eng. and Design* 33 (1975) 50.
- [25] B. Canut, S.M.M. Ramos, P. Thevenard, N. Moncoffre, A. Benyagoub, G. Marest, A. Meftah, M. Toulemonde and F. Studer, *Nucl. Instr. and Meth. B* 80/81 (1993) 1114.
- [26] M.P.R. Waligorski, R.N. Hamm and R. Katz, *Nucl. Tracks Radiat. Meas.* 11 (1986) 309.
- [27] R. Spohr, in: *Ion tracks and microtechnology: principles and applications*, ed. K. Bethge (Vieweg, 1990) p. 118.
- [28] M. Toulemonde, C. Dufour and E. Paumier, *Phys. Rev. B* 46 (1992) 14362.